Proc. SPIE 2968 (1997) 180 - 185

X-ray absorption spectroscopy study of the local environment around tungsten and molybdenum ions in tungsten-phosphate and molybdenum-phosphate glasses

A. Kuzmin and J. Purans

Institute of Solid State Physics, University of Latvia, 8 Kengaraga str., LV-1063 Riga, Latvia

ABSTRACT

X-ray absorption spectroscopy (XAS) was used to study the local environment around tungsten and molybdenum ions in $BaO-P_2O_5-WO_3$ and $CaO-P_2O_5-MoO_3$ glasses having different composition of WO_3 and MoO_3 oxides. The W $L_{1,3}$ and Mo K edges x-ray absorption spectra were measured in transmission mode at room temperature using the synchrotron radiation emitted by the ADONE and LURE DCI storage rings, respectively. The analysis of x-ray absorption near edge structure (XANES) and extended x-ray absorption fine structure (EXAFS) in glasses was performed in comparison with the results for a number of crystalline WO_3, $CaWO_4$, $Na_{0.66}WO_3$, α-MoO_3, β-MoO_3 and amorphous a-WO_3, a-MoO_3 compounds. The results of the EXAFS modelling by two different methods ((1) multi-shell best-fit procedure within harmonic approximation and (2) model-independent radial distribution function approach) allowed us to extract detailed structural information on the first coordination shell of metal (W or Mo) ions. Using the obtained data together with the information given by XRD, EPR and optical spectroscopies, we propose the model of incorporation of W and Mo ions within the glass network.

Keywords: XAS, XANES, EXAFS, W L_1 and L_3 edges, Mo K-edge, oxide glasses, electrochromic materials

1. INTRODUCTION

Tungsten-phosphate and molybdenum-phosphate glasses belong to a group of glasses which incorporate distorted octahedral structural units [MeO_6] (Me=W, Mo) within the glass network and whose structure is still not well understood.[1-3] Besides they exhibit interesting electrochromic properties and high ionic conductivity that makes them potential materials for electro-optical applications.[3,4] Recent use of the x-ray absorption spectroscopy to study tungsten-phosphate glasses showed possibility to obtain original and complementary to other experimental techniques information on the local environment around tungsten ions.[3,4] In this work we present an accurate EXAFS study of the short range order of tungsten and molybdenum ions in phosphate glasses using conventional multi-shell harmonic approximation and model-independent radial distribution function (RDF) approach, developed recently by one of us.[5]

2. EXPERIMENTAL AND DATA ANALYSIS

The tungsten-phosphate and molybdenum-phosphate glasses had the following compositions (in mol.%): 40 BaO-40 P_2O_5-20 WO_3 (20%WO_3), 30 BaO-30 P_2O_5-40 WO_3 (40%WO_3), 20 BaO-20 P_2O_5-60 WO_3 (60%WO_3), 34 P_2O_5-66 WO_3 (66%WO_3), 45 CaO-45 P_2O_5-10 MoO_3 (10%MoO_3), 40 CaO-40 P_2O_5-20 MoO_3 (20%MoO_3), 30 CaO-30 P_2O_5-40 MoO_3 (40%MoO_3) and 20 CaO-20 P_2O_5-60 MoO_3 (60%MoO_3). A set of reference compounds was also used: polycrystalline powders of WO_3, $Na_{0.66}WO_3$, $CaWO_4$ and α-MoO_3, polycrystalline thin-film of β-MoO_3 and amorphous thin-films of a-WO_3 and a-MoO_3.

X-ray absorption spectra (XAS) (Fig. 1) of glasses and reference compounds were measured in transmission mode at the W $L_{1,3}$ and Mo K edges using a standard setup of the ADONE PWA-BX1 wiggler beam line, equipped with the Si(220) channel-cut crystal monochromator and two ionization chambers containing krypton gas, and the LURE DCI EXAFS-3 beam line, equipped with the Si(311) double-crystal monochromator and two ionization chambers containing argon gas, respectively. The storage rings ADONE and DCI operated at the average energy 1.5 and 1.85 GeV and the maximum stored current about 20÷50 and 250÷350 mA, respectively. All measurements were performed at room temperature. The experimental resolution was estimated about 1.5 eV at the W L-edges and about 4 eV at the Mo K-edge. The samples had a thickness x leading to the absorption jump Δmx about 0.5÷1.3 at the W L-edges and 0.7÷1.9 at the Mo K-edge**.**

The XAS were treated by the "EDA" software package following the standard procedure.[5]

The E_0 position, defining the zero wave vector (k=0), was set at 5 eV above the white line (WL) for the W L_3-edge or the pre-edge shoulder, which corresponds to the WL, for the W L_1 and Mo K edges according to the procedure utilized by us earlier[6] (see Fig. 1). This energy point corresponds approximately to the position of the inner core photoemission threshold (vacuum level) and its correct choice is essential to align experimental and theoretical spectra. The extracted experimental extended x-ray absorption fine structure (EXAFS) signals (Figs. 2(a) and 3(a)) were defined as $c(k)=(m(E)-m_b(E)-m_0(E))/\underline{m}_0(E)$ where $k=((2m_e/\hbar^2)\Delta E)^{1/2}$ and $m(E)$ is the experimental absorption

coefficient, $m_b(E)$ the background contribution determined by an extrapolation of the pre-edge XAS part of $m(E)$ above the absorption edge, $m_0(E)$ the atomic-like contribution or the EXAFS signal zero-line, $\underline{m}_0(E)$ the normalization function, m_e the electron mass, $\hbar$ the Planck's constant and $\Delta E=E-E_0$ the photoelectron kinetic energy.[5]

The EXAFS signal from a coordination shell, located between R_{min} and R_{max} and consisting of only one type of atoms, is given within the spherical-wave approximation (SWA) by

$$c(k) = S_0^2 \int_{R_{min}}^{R_{max}} \frac{G(R)}{kR^2} F(p,k,R)\sin(2kR + F(p,k,R))\,\mathrm{d}R \qquad (1)$$

where S_0^2 is the scale factor taking into account amplitude damping due to the multielectron effects; R is the interatomic distance; $G(R) = 4\pi R^2 r_0 g_2(R)$ is the radial distribution function (r_0 is the average density and $g_2(R)$ is the pair-distribution function); $F(\pi,k,R)$ is the backscattering amplitude of the photoelectron due to the atoms located at the distance R from the photoabsorber and $F(\pi,k,R) = y(\pi,k,R) + 2d_l\,(k) - l\pi$ is the phase shift containing contributions from the photoabsorber $2d_l\,(k)$ and the backscatterer $y(\pi,k,R)$ (l is the angular momentum of the photoelectron, l=1 for the K and L_1 edges and l=2 or 0 for the $L_{2,3}$-edges). In the present notation the amplitude function $F(\pi,k,R)$ contains intrinsic the damping factor due to the mean free path of the photoelectron assuming that $F(\pi,k,R)$ is calculated using a complex exchange-correlation potential of the Hedin-Lundqvist type.[7,8] In this work the functions $F(\pi,k,R)$ and $F(\pi,k,R)$ for the W-O and Mo-O atom pairs were calculated by the FEFF code[8] with the muffin-tin radii equal to 1.1 Å for the absorber (W, Mo) and 0.9 Å for the neighbouring oxygen atoms. The RDF $G(R)$ in (1) corresponds to the number of atoms located in the spherical shell around the photoabsorber between R and R + dR so that the average number N of atoms (the coordination number) located in the region between R_{min} and R_{max} is given by the integral $N = \int_{R_{min}}^{R_{max}} G(R)\mathrm{d}R$.

It is easy to see from the form of Eq. (1) that the conventional Fourier filtering technique can be applied to the EXAFS signal to single out the contribution from a particular coordination shell. The Fourier transforms (FT) of the EXAFS signals $c(k)k^2$, multiplied by a Kaiser-Bessel window to reduce the influence of truncation effects in k-space, were calculated, depending on the compound, in the k-range from 0.5÷0.7 to 14÷16 Å^{-1}(Figs. 2(b) and 3(b)). The EXAFS signals, related to the first peak in FT's, which corresponds to the first coordination shell of tungsten or molybdenum ions, were singled out by the back-FT procedure.

Thus obtained first-shell EXAFS signals were utilized in the best-fit procedure using two different methods: (1) the multi-shell single-scattering model within harmonic approximation and (2) the model-independent radial distribution function (RDF) approach.[5] In the first method, the RDF $G(R)$ is sought as a sum of the q Gaussian lines

$$G(R) = \sum_{i=1}^{q} \frac{N_i}{\sqrt{2p\,s_i^2}} \exp\left(-\left(R - R_i\right)^2 \Big/ 2s_i^2\right) \qquad (2)$$

where N_i, R_i and s_I^2 are the fitting parameters. In the second method, the RDF $G(R)$ is described by a histogram with an appropriate step in R-space and the constrain conditions of non-negativity and smoothness imposed on the $G(R)$ shape. To compare the results of two methods, the model-independent RDF's, obtained by the second approach, were decomposed into a set of Gaussian lines whose parameters were found to be in good agreement with the ones obtained by the first method (Figs. 4 and 5).

One should point out that according to the Nyquist criterion,[9] the total number of the fitting parameters $N_{fit} = 3q$ (where q is the number of Gaussians in Eq. (2)) used in the Gaussian model should be less than the number of independent data points[9] $N_{ind} = 2\Delta k\Delta R / \pi + 2$ where Δk and ΔR are, respectively, the widths in k and R space used in the fit. Thus, the Nyquist criterion defines the *maximum* quantity of information which can be contained within a spectral range. On practice, the quantity of structural information in the experimental data is again limited at least by the structure itself and by the presence of noise therefore to distinguish between structural models the dispersive analysis based on the Fisher's $F_{0.95\%}$-test should be used. In this work, the total number of the fitting parameters and the obtained results satisfy both to the Nyquist criterion and to the Fisher's $F_{0.95\%}$-test.[10] More details of the data analysis can be found in Refs. 5 and 10.

3. RESULTS AND DISCUSSION

3.1 XANES

The XANES signals at the W L_3-edge contain a strong resonance - the so-called "white line" (WL), located just below the continuum threshold E_0 (Fig. 1): it corresponds to the dipole-allowed transition from the $2p_{3/2}$(W) level into a quasi-bound 5*d*(W) + 2*p*(O) mixed-state.[4] The same final state is probed by the excitation of the 2*s*(W) electron at the L_1-edge, however, in this case the intensity of the transition depends strongly on the local symmetry and the degree of the *pd*-mixing (similar transition 1*s*(Mo) → 4*d*(Mo) + 2*p*(O) occurs for the Mo K-edge). The transition is dipole-forbidden in regular octahedron, having an inversion center, but becomes allowed in distorted octahedron (WO_3) and in tetrahedron ($CaWO_4$). Thus, the intensity of the peak (shoulder) below the continuum threshold at the K or L_1 edge allows to estimate roughly the coordination and the degree of distortion in the first coordination shell. A comparison of the XANES signals suggests that in glasses, both W and Mo ions are located in strongly distorted octahedral-like coordination.

3.1 EXAFS

The qualitative results of the XANES analysis agree well with the quantitative data obtained from EXAFS. The simulations of the first-shell EXAFS signals in BaO-P_2O_5-WO_3 glasses by two methods, mentioned above, suggests that the RDF's around tungsten (Fig. 4(a)) are composed of two groups of 3 oxygen ions each, located at ~1.73 and ~2.02 Å. Note that in 60%WO_3-glass, there are octahedra of two types, distorted as 3:3 (~70%) and 4:2 (~30%): the latter distortion is similar to the one in crystalline WO_3. Close RDF's were found in CaO-P_2O_5-MoO_3 glasses (Fig. 5(a)), however, here the RDF peak of the distant group of oxygen ions is strongly asymmetric with a tail at long distances. As a result, the local surrounding of molybdenum can be approximated by three groups of oxygens consisting of 3, 2 and 1 atoms at ~1.68, ~1.98 and ~2.11 Å, respectively. Note that in the 66%WO_3-glass without BaO, the 1st-shell is splitted into two groups of 2 and 4 oxygen ions at ~1.72 and ~1.95 Å. Thus, the type of the first-shell distortion in phosphate glasses differs from the one in the reference crystals and amorphous thin films (Table 1) but is similar to the one observed in monophosphate tungsten bronzes:[11] it can be attributed to the *off-centre* displacement of W or Mo ions in the ⟨111⟩ directions. Note that in pure crystalline and amorphous MeO_3 compounds, W or Mo ions are displaced *off-centre* in the ⟨110⟩ directions (Table 1).

The degree of the [MeO_6] distortion Δ was estimated from the RDF's using the formula $\Delta = \langle|R - \langle R\rangle|\rangle$.[12] Note that in the glasses, Δ decreases with increasing MeO_3 content (Fig. 6(a)) that is attributed to a decrease of the number of long Me OPO_3 bonds, and, besides, Δ is large in the molybdenum

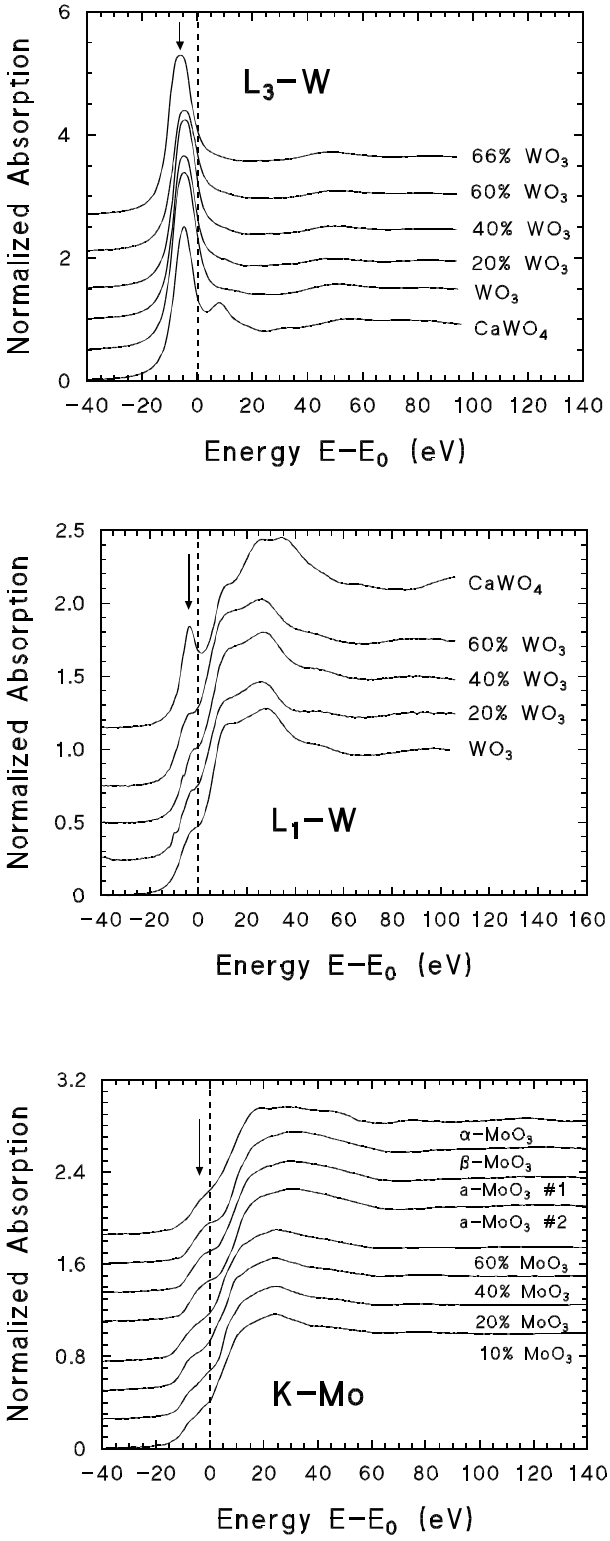

Fig. 1. XANES signals at the W $L_{1,3}$ and Mo K edges in glasses and reference compounds. The positions of the white lines (WL) are indicated by arrows. Note the increase of the WL intensity at the L_1 and K edges with increasing [MeO_6] distortion (Me = W, Mo).

Proc. SPIE 2968 (1997) 180 - 185

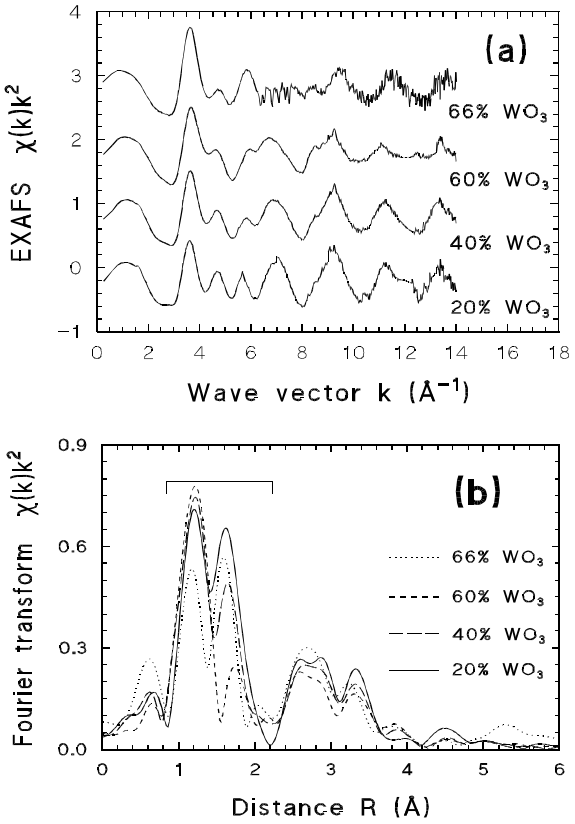

Fig. 2. EXAFS signals and their FT's at the W L_3-edge. The region of the first shell is indicated by solid bracket.

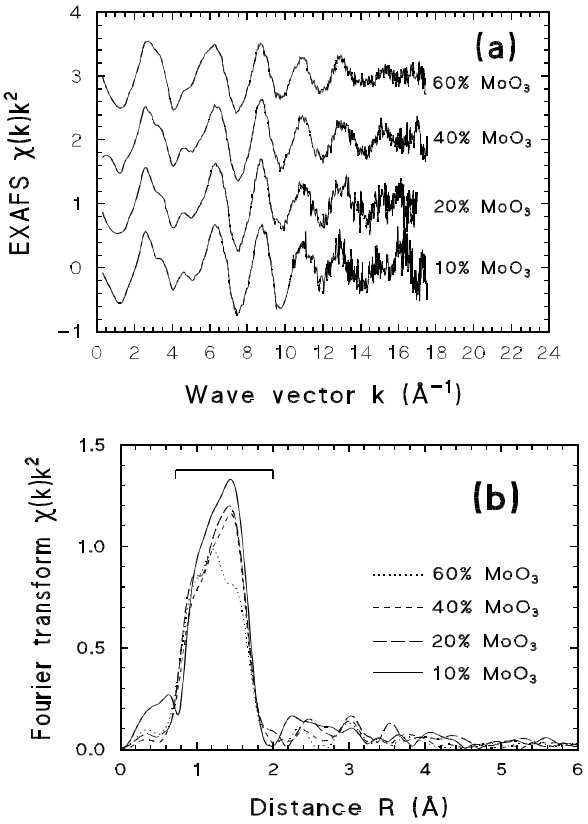

Fig. 3. EXAFS signals and their FT's at the Mo K-edge. The region of the first shell is indicated by solid bracket.

glasses and oxides (Fig. 6(a) and Table 1). In tungsten containing reference compounds, the values of Δ agree with the ones from diffraction studies and correlate with the valence state of tungsten ions:[12] this dependence allows to estimate the valency of W in glasses (Fig. 6(b)). The obtained results suggest that in spite of a signal from the W^{5+} d^1- ions has been detected by electron paramagnetic resonance (EPR) spectroscopy[13] in these glasses, the total amount of W^{5+} ions is sufficiently small to be revealed in the EXAFS signal.

The peaks in FT's beyond the first one at 2.1÷4.2 Å (Fig. 2(b) and 3(b)) remain nearly unchanged despite the modifications occurring within the first shell of metal ions: these peaks are attributed mainly to the multiple-scattering (MS) effects within the first shell octahedron,[4,6,10] however, the single-scattering (SS) signals from phosphorus and tungsten (molybdenum) atoms, located in the second shell, contribute also in that region. The origin of the peaks at 2.1÷4.2 Å is explained by the following reasons. First, it is known[14] that the MS contribution from an octahedron is less sensitive to its distortion than the SS one: this explains the stability of the peaks shape, especially, in the tungsten glasses where the MS contribution dominates the SS one. Second, it is also known[6,14] that the MS contribution depends strongly on the photoelectron angular momentum (the absorption edge type), especially, in the case of the double-scattering paths $Me_0 \rightarrow O_1 \rightarrow O_2 \rightarrow Me_0$ with $\angle O_1Me_0O_2$ 90° whose contribution is smaller in the K,L_1-EXAFS than in $L_{2,3}$-EXAFS: this explains why the peaks magnitude in the tungsten glasses is larger than in the molybdenum glasses (compare Figs. 2(b) and 3(b)) where the relative weight of the signals from P and Mo atoms in the second shell increases compared to the MS contribution.[10]

Finally, the results of the XAS analysis suggest that in tungsten-phosphate and molybdenum-phosphate glasses, the local environment around tungsten and molybdenum ions is similar enough in sense that they are located preferentially at the off-center positions within distorted octahedra [MeO_6] (Me=W, Mo). The [MeO_6] octahedra are connected mainly by corners to [PO_4] and other [MeO_6] groups resulting in the formation of chains or blocks of [MeO_6] octahedra which are responsible for the electronic and magnetic properties of the glasses.[10] The latter conclusion is consistent with the results of the EPR spectroscopy.[13]

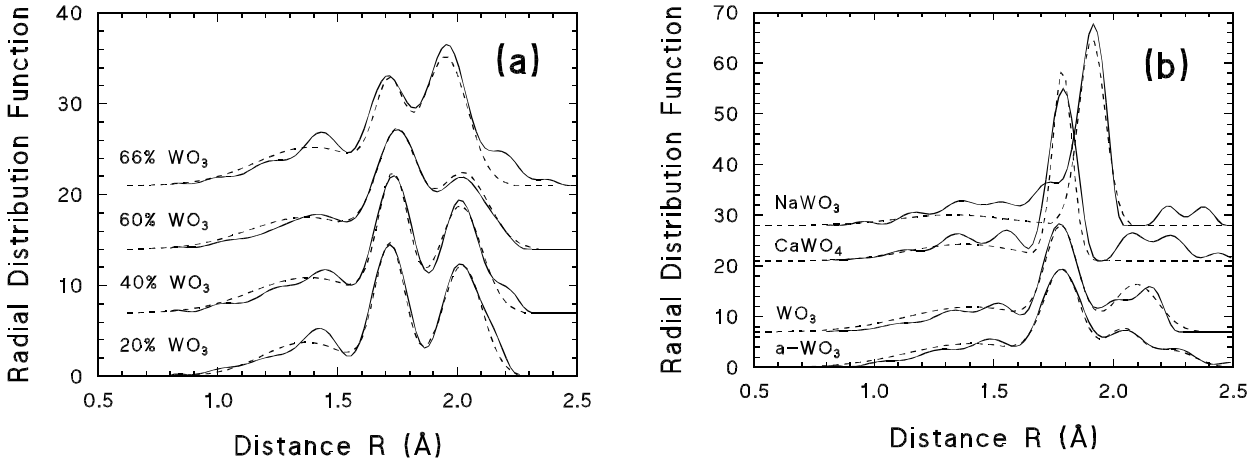

Fig. 4. RDF G(R) around tungsten ions in (a) BaO-P_2O_5-WO_3 and P_2O_5-WO_3 glasses; (b) reference compounds. Solid curves: RDF's calculated by the model-independent method (Eq. (1)). Dashed curves: RDF's calculated by the multi-shell single-scattering model within harmonic approximation (Eqs. (1) and (2)).

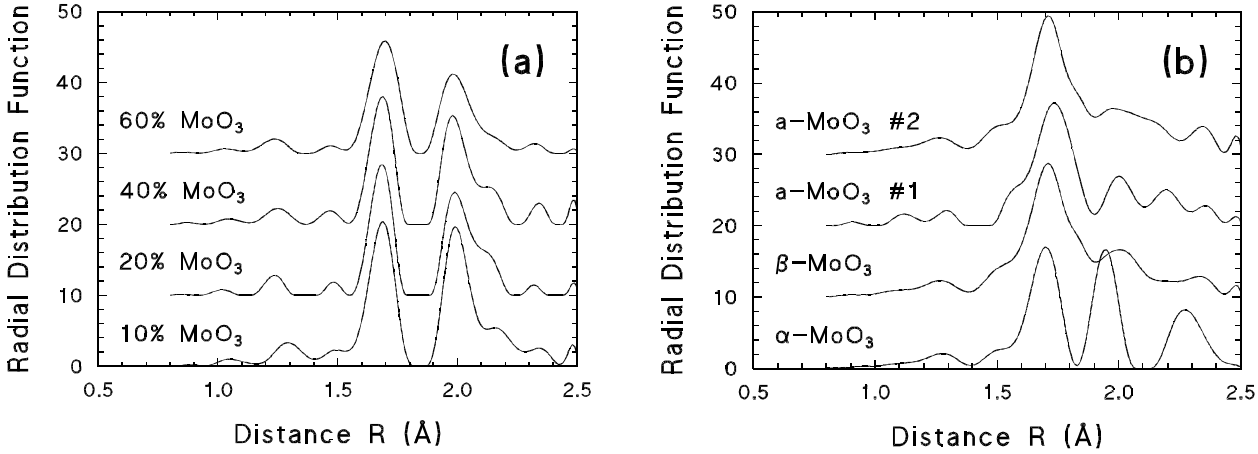

Fig. 5. RDF G(R) around molybdenum ions in (a) CaO-P_2O_5-MoO_3 glasses and (b) reference compounds. RDF's were calculated by the model-independent method (Eq. (1)).

4. ACKNOWLEDGMENTS

The authors are grateful to the staff of the ADONE PWA laboratory (Frascati, Italy) and of the LURE DCI EXAFS-3 beam line (Orsay, France) for the support of the experiments. This work was also supported in part by the International Science Foundation, Grants No. LF8000 and LJ8100.

5. REFERENCES

1. U. Selvaraj and K.J. Rao, "ESR and optical studies of Mo^{5+} and W^{5+} ions in phosphomolybdate and phosphotungstate glasses," *Chem. Phys.* **123,** 141-150 (1988).

2. B. Bridge and N.D. Patel, "The elastic constants and structure of the vitreous system Mo-P-O," *J. Mater. Sci.* **21,** 1187-1205 (1986).

3. F. Studer, A. Lebail and B. Raveau, "Local environment of tungsten in mixed valence tungsten phosphate glasses: an EXAFS study," *J. Solid State Chem.* **63**, 414-423 (1986).

4. A. Balerna, E. Bernieri , E. Burattini, A. Kuzmin and J. Purans, "Study of the local environment around tungsten in

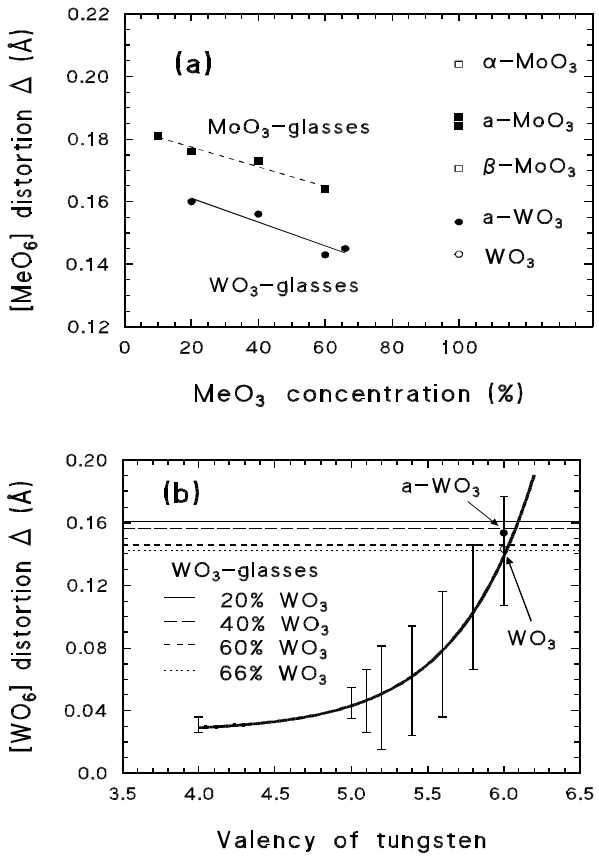

Fig. 6. (a) Distortion Δ of the MeO_6 (Me=W,Mo) octahedron vs. MeO_3 concentration. (b) Dependence of the WO_6 distortion Δ from the valence state of tungsten. Solid line represents results from Ref. 12.

Table 1. Distortion Δ of the first shell and its type in glasses and reference compounds according to the EXAFS data. The direction of the *off-centre* displacement is also given.

Compound	Type of distortion	Direction of displacement	Δ (Å)
$CaWO_4$	4		0.045
$Na_{0.66}WO_3$	6		0.048
WO_3	4 : 2	⟨110⟩	0.143
a-WO_3	4 : 1 : 1	⟨110⟩	0.154
20% WO_3	3 : 3	⟨111⟩	0.160
40% WO_3	3 : 3	⟨111⟩	0.156
60% WO_3	3 : 3 (~70%)	⟨111⟩	0.143
	4 : 2 (~30%)	⟨110⟩	
66% WO_3	2 : 4		0.145
α-MoO_3	2 : 2 : 2	⟨110⟩	0.204
β-MoO_3	4 : 2	⟨110⟩	0.171
a-MoO_3 #1	4 : 1 : 1	⟨110⟩	0.187
a-MoO_3 #2	4 : 1 : 1	⟨110⟩	0.184
10% MoO_3	3 : 2 : 1	⟨111⟩	0.181
20% MoO_3	3 : 2 : 1	⟨111⟩	0.176
40% MoO_3	3 : 2 : 1	⟨111⟩	0.172
60% MoO_3	3 : 2 : 1	⟨111⟩	0.164

mixed valence barium-tungsten-phosphate glasses by x-ray absorption spectroscopy," Proc. XVI Inter. Congress on Glass, Madrid, 1992, vol. 3, pp. 347-352.

5. A. Kuzmin, "EDA: EXAFS data analysis software package," *Physica B* **208&209**, 175-176 (1995); A. Kuzmin, *J.Phys. IV France* (1997) (to be published).

6. A. Kuzmin, J. Purans, M. Benfatto and C.R. Natoli, "X-ray-absorption study of rhenium L_3 and L_1 edges in ReO_3: Multiple-scattering approach," *Phys. Rev. B* **47,** 2480-2486 (1993).

7. L. Hedin and B.I. Lundqvist, "Explicit local exchange-correlation potentials," *J. Phys. C: Solid State Phys.* **4**, 2064-2083 (1971).

8. J. Mustre de Leon, J.J. Rehr, S.I. Zabinsky, and R.C. Albers, "Ab initio curved-wave x-ray-absorption fine structure," *Phys. Rev. B* **44**, 4146-4156 (1991).

9. E.A. Stern, "Number of relevant independent points in x-ray-absorption fine-structure spectra," *Phys. Rev. B* **48**, 9825-9827 (1993).

10. A. Kuzmin and J. Purans, *J. Non-Cryst. Solids* (1997) (to be published).

11. P. Labbe, M. Goreaud and B. Raveau, "Monophosphate tungsten bronzes with pentagonal tunnels $(PO_2)_4(WO_3)_{2m}$: Structure of two even-*m* members $P_4W_{12}O_{44}$ (*m*=6) and $P_4W_{16}O_{56}$ (*m*=8)," *J. Solid State Chem.* **61**, 324-331 (1986).

12. B. Domengès, N.K. McGuire and M. O'Keeffe, "Bond lengths and valences in tungsten oxide," *J. Solid State Chem.* **56**, 94-100 (1985).

13. P.D. Cikmach, Ph.D. Thesis (University of Latvia, Riga, 1985) pp.196-201 [in Russian].

14. A. Kuzmin and R. Grisenti, "Evaluation of multiple-scattering contribution in extended x-ray absorption fine structure for MO_4 and MO_6 clusters," *Phil. Mag. B* **70,** 1161-1175 (1994).